Engineering 6 (2020) 904–912

Contents lists available at ScienceDirect

Engineering

journal homepage: www.elsevier.com/locate/eng

Research
Geodesy and Survey Engineering—Article

Precise Orbit Determination for the FY-3C Satellite Using Onboard BDS and GPS Observations from 2013, 2015, and 2017

Xingxing Li [a,b,*], Keke Zhang [a], Xiangguang Meng [c,d,*], Wei Zhang [a], Qian Zhang [a], Xiaohong Zhang [a], Xin Li [a]

[a] School of Geodesy and Geomatics, Wuhan University, Wuhan 430079, China
[b] German Research Centre for Geosciences (GFZ), Potsdam 14473, Germany
[c] National Space Science Center, Chinese Academy of Sciences, Beijing 100190, China
[d] Beijing Key Laboratory of Space Environment Exploration, Beijing 100190, China

ARTICLE INFO

Article history:
Received 26 July 2018
Revised 13 November 2018
Accepted 25 March 2019
Available online 5 September 2019

Keywords:
FengYun-3C
LEO precise orbit determination (POD)
Onboard BDS and GPS
BDS code bias
BDS/GPS combined POD

ABSTRACT

Using the FengYun-3C (FY-3C) onboard BeiDou Navigation Satellite System (BDS) and Global Positioning System (GPS) data from 2013 to 2017, this study investigates the performance and contribution of BDS to precise orbit determination (POD) for a low-Earth orbit (LEO). The overlap comparison result indicates that code bias correction of BDS can improve the POD accuracy by 12.4%. The multi-year averaged one-dimensional (1D) root mean square (RMS) of the overlapping orbit differences (OODs) for the GPS-only solution is 2.0, 1.7, and 1.5 cm, respectively, during the 2013, 2015, and 2017 periods. The 1D RMS for the BDS-only solution is 150.9, 115.0, and 47.4 cm, respectively, during the 2013, 2015, and 2017 periods, which is much worse than the GPS-only solution due to the regional system of BDS and the few BDS channels of the FY-3C receiver. For the BDS and GPS combined solution (also known as the GC combined solution), the averaged 1D RMS is 2.5, 2.3, and 1.6 cm, respectively, in 2013, 2015, and 2017, while the GC combined POD presents a significant accuracy improvement after the exclusion of geostationary Earth orbit (GEO) satellites. The main reason for the improvement seen after this exclusion is the unfavorable satellite tracking geometry and poor orbit accuracy of GEO satellites. The accuracy of BDS-only and GC combined solutions have gradually improved from 2013 to 2017, thanks to improvements in the accuracy of International GNSS Service (IGS) orbit and clock products in recent years, especially the availability of a high-frequency satellite clock product (30 s sampling interval) since 2015. Moreover, the GC POD (without GEO) was able to achieve slightly better accuracy than the GPS-only POD in 2017, indicating that the fusion of BDS and GPS observations can improve the accuracy of LEO POD. GC combined POD can significantly improve the reliability of LEO POD, simply due to system redundancy. An increased contribution of BDS to LEO POD can be expected with the launch of more BDS satellites and with further improvements in the accuracy of BDS satellite products in the near future.

© 2020 THE AUTHORS. Published by Elsevier LTD on behalf of Chinese Academy of Engineering and Higher Education Press Limited Company. This is an open access article under the CC BY-NC-ND license (http://creativecommons.org/licenses/by-nc-nd/4.0/).

1. Introduction

Over the past two decades, low-Earth orbits (LEOs) have been utilized in a broad range of fascinating missions for oceanography, solid-Earth physics, and sea-level research, which usually has a centimeter-level orbit requirement. As shown by the successful use of Global Positioning System (GPS)-based precise orbit determination (POD) for the TOPEX/Poseidon satellite [1], the onboard GPS technique makes it possible to obtain a high-precision orbit result and has been widely used for many missions. The existing results show that POD on the level of a few centimeters can be obtained with onboard GPS data for Earth-observation satellite missions, such as GRACE, GOCE, and Swarm [2–4].

The BeiDou Navigation Satellite System (BDS) is independently developed and operated by China. By the end of 2012, BDS had the ability to provide regional services. At present, there are a total of 34 BDS satellites in orbit, including 15 BDS-2 satellites (six geostationary Earth orbit (GEO) satellites, six inclined geosynchronous orbit (IGSO) satellites, and three medium-Earth orbit (MEO) satellites) and 19 BDS-3 satellites (two IGSO satellites and 17 MEO satellites). Numerous studies have been carried out on BDS-2 satellites, on topics such as BDS POD [5], precise point positioning (PPP)

* Corresponding authors.
E-mail addresses: xxli@sgg.whu.edu.cn (X. Li), xgmeng@nssc.ac.cn (X. Meng).

https://doi.org/10.1016/j.eng.2019.09.001
2095-8099/© 2020 THE AUTHORS. Published by Elsevier LTD on behalf of Chinese Academy of Engineering and Higher Education Press Limited Company.
This is an open access article under the CC BY-NC-ND license (http://creativecommons.org/licenses/by-nc-nd/4.0/).

[6,7], and global navigation satellite system (GNSS) meteorology [8–10].

In 2013, the FengYun-3C (FY-3C) satellite was launched by the China Meteorological Administration/National Satellite Meteorological Center (CMA/NSMC) as a new generation of weather satellite to monitor the Earth's atmosphere, climatic prediction, and forecast. The FY-3C satellite carries a GNSS occultation sounder (GNOS) instrument, which can track BDS and GPS signals simultaneously. The onboard BDS and GPS data of the FY-3C provides a great opportunity to investigate the performance and contribution of BDS to LEO POD. Several researchers have reported initial results for FY-3C POD. Using a month of FY-3C onboard data, Li et al. [11] carried out BDS-only and BDS and GPS (GC) combined POD for the FY-3C. The orbit overlap comparison result shows that the BDS-only POD can reach a three-dimensional (3D) root mean square (RMS) of 32.67 cm, while the 3D RMS of the GC combined POD is 3.86 cm, which is worse than the GPS-only solution. However, the GC combined POD can reach a similar precision to the GPS POD with a 3D RMS of 2.73 cm when BDS GEO satellites are excluded. Xiong et al. [12] achieved real-time POD with an accuracy of 1.24 m for the FY-3C using BDS and GPS code data. Zhao et al. [13] utilized the estimated POD of the FY-3C and regional station observations to enhance the BDS orbit, and improved the BDS orbit accuracy from 354.3 to 63.1 cm for GEO, 22.7 to 20.0 cm for IGSO, and 20.9 to 16.7 cm for MEO satellites.

In this paper, we focus on the performance and contribution of BDS to LEO POD. Several strategies are designed to analyze and evaluate the FY-3C POD in detail, including the impact of BDS satellite-induced code bias on POD, FY-3C POD with different BDS orbit and clock products, BDS-only POD, and GC combined POD for the FY-3C. POD performance for the FY-3C over a long time-span is also investigated. This paper is organized as follows. In Section 2, we give an overview of the FY-3C satellite and analyze the availability of FY-3C onboard data. Section 3 focuses on the method and strategy to estimate orbit parameters. In Section 4, we investigate the impact of BDS satellite-induced code bias on LEO POD. Next, the POD for the FY-3C with different strategies is assessed comprehensively through an orbit overlap comparison and residual analysis. Finally, Section 5 provides a summary of our results and corresponding conclusions.

2. The FY-3C platform and data collection

The FY-3C is the first operational satellite of the Chinese FengYun-3 series and has an orbit altitude of 836 km. Its orbit inclination is 98.75° and the total weight of the spacecraft in orbit is 2405.7 kg [11]. To fulfill the requirement of radio occultation observation and POD, the FY-3C is equipped with a GNOS instrument, which is designed and manufactured by Center for Space Science and Applied Research (CSSAR). Three antennas are mounted on the GNOS receiver: the positioning antenna (PA), the rising occultation antenna, and the setting occultation antenna [14]. The PA of the GNOS receiver has four BDS and eight GPS tracking channels. However, up to six BDS satellites and more than eight GPS satellites can be observed simultaneously through the PA by GNOS, because the PA can utilize the idle channels preassigned for the occultation antenna [11]. The onboard GNSS data from the PA are used for the navigation and POD of the FY-3C.

This study representatively analyzes the onboard BDS and GPS data with a 1 s sample interval for the FY-3C during day of year (DOY) 316–365 in 2013, DOY 96–145 in 2015, and DOY 61–110 in 2017. The available data include C2I, C7I code and L2I, L7I carrier phase observations for the BDS B1 and B2 frequencies, respectively, and C1C, C2P code and L1C, L2P carrier phase observations for the GPS L1 and L2 frequencies, respectively.

In order to assess the availability of FY-3C onboard GNSS data, the numbers of BDS and GPS observations from different periods were counted. Fig. 1(a) presents the daily average number of observations for BDS and GPS based on the selected data period in different years. It can be seen that for GPS, the C1C code and L1C carrier phase observations are almost comparable in amount to the C2P code and L2P carrier phase observations. Although there is no obvious reduction in the number of GPS observations from 2015 to 2017, the observation number in 2013 is slightly less than those in 2015 and 2017. For BDS satellites, the number of C2I and L2I observations is slightly greater than that of C7I and L7I. Unlike the GPS, a noticeable reduction in the quantity of BDS observations can be observed from 2013 to 2017.

We then computed the effectiveness for both BDS and GPS; the results are presented in Fig. 1(b). Effectiveness is defined as the ratio of lost epochs with no satellites tracked to all epochs for every day. The effectiveness for GPS is less than 8% for most days in 2013, but is close to zero in 2015 and 2017, except for DOY 85 in 2017. In

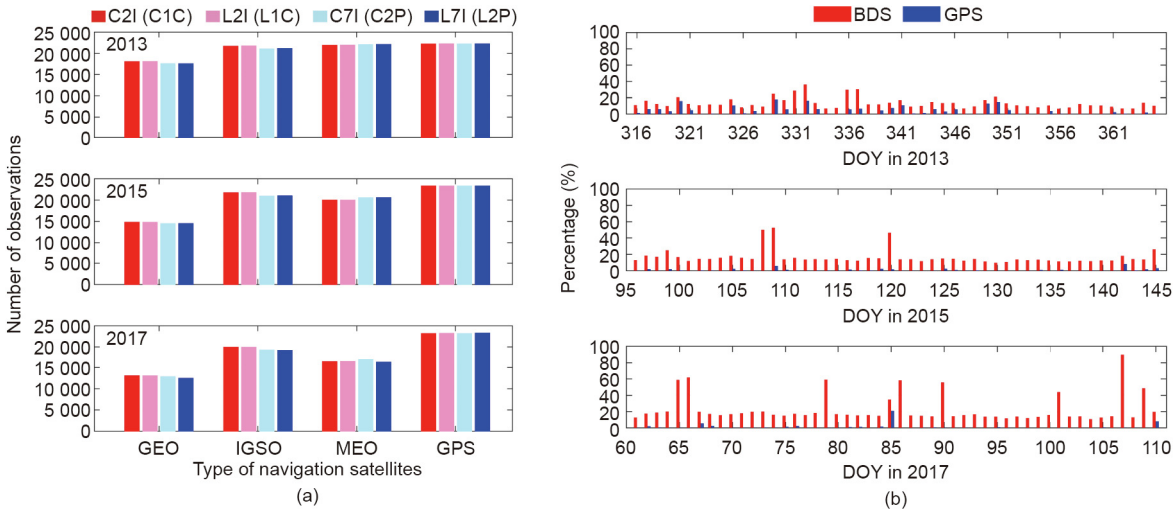

Fig. 1. (a) Daily average number of different types of observations for BDS and GPS satellites; (b) daily effectiveness of BDS and GPS onboard data.

contrast, the effectiveness of BDS is greater than 10% for most days; on some days, such as DOY 109 and 120 in 2015 and DOY 65 and 66 in 2017, it even exceeds 50%, which has a severe influence on the BDS-only POD for the FY-3C. The data loss for BDS increases gradually from 2013 to 2017, leading to a reduction in the number of BDS observations. However, the specific reason for the increase in BDS data loss is unclear, and requires further investigation. We infer that the increase in BDS data loss is associated with the aging of the space-borne GNOS receiver.

3. POD method and strategy

Four FY-3C POD schemes—namely, BDS-only, GPS-only, GC (with GEO), and GC (without GEO)—were performed using the reduced-dynamic approach based on the data from 2013 to 2017. Table 1 lists information on the precise orbit and clock products for GPS and BDS. It should be pointed out that no analysis center provided Multi-GNSS Experiment (MGEX) orbit and clock products containing GPS and BDS simultaneously in 2013, so the precise orbit and clock products used in 2013 are combined from the products provided by the International GNSS Service (IGS) and Wuhan University (WHU). Note that the IGS and WHU orbit products had different intervals (15 min for IGS and 5 min for WHU) in 2013. We simply merged the orbit and clock of GPS and BDS at the same epoch. In other words, the interval of the merged orbit and clock is 15 and 5 min, respectively. It is worth noting that the sampling intervals of the MGEX orbit and clock products from the German Research Centre for Geosciences (GFZ) have changed since DOY 123 in 2015.

Table 2 provides the details of the POD strategy for the FY-3C. We selected an arc length of 30 h with 6 h of overlap between the adjacent orbit arcs, from 21:00 on the previous day to 3:00 on the next day. The final orbit and clock products from IGS [15], WHU [16], and GFZ [17] are used. The GPS phase correction offset (PCO) and phase correction variation (PCV) are taken into account according to the IGS model from "igs08.atx" [18] and "igs14.atx" [19]. For BDS, the MGEX-recommended PCO values are used and the PCV is omitted for 2013, while the PCO and PCV correction estimated by European Space Agency (ESA) [20] are used for 2015 and 2017. We employ the same PCO values as Li et al. [11] to correct the PCO for the FY-3C, and the PCV of the FY-3C receiver is ignored. During POD processing, an equal weight strategy is applied for GPS, BDS IGSO, and MEO observations, while the weight of the GEO observations is set to two fifths of the IGSO and MEO observations to reduce the negative influence of GEO orbit products.

For LEO, the main non-conservation forces include the atmospheric drag, solar radiation pressure, and Earth radiation pressure, which are all related to the geometrical shape of the satellite. Due to a lack of detailed geometrical information for the FY-3C, the solar radiation pressure is computed by the Box-wing model with a simplified geometric model of the FY-3C. Based on information about the shape of the satellite, the atmospheric drag is calculated, with the atmosphere density being computed by DTM94 [21]; in addition, the drag scale coefficient is estimated as a piecewise constant parameter in order to partly compensate for the error due to the simplified geometric model. The Earth radiation pressure is not considered in the POD for the FY-3C in this study.

Table 1
The precise products used for FY-3C POD.

Year	Institution	Orbit products interval	Clock products interval
2013	IGS + WHU	15 min	5 min
2015	GFZ	15 min/5 min	5 min/30 s
2017	GFZ	5 min	30 s

IGS: International GNSS Service; WHU: Wuhan University; GFZ: German Research Centre for Geosciences.

Table 2
Summary of POD strategy for the FY-3C.

Model	Description
Observation model	
Observation	Un-differenced ionosphere-free code & phase
Interval	10 s
POD arc length	30 h
Elevation cut-off angle	1°
GPS satellite PCO & PCV	igs08.atx for 2013 and 2015, igs14.atx for 2017
BDS satellite PCO & PCV	MGEX-recommended PCO for 2013, PCO and PCV model from ESA for 2015 and 2017
GNOS PCO	Corrected
GNOS PCV	Not considered
Satellite attitude	Nominal
Weighting strategy	Weighting ratio for GPS, BDS IGSO, MEO, GEO observations is 5:5:5:2
Dynamics model	
Earth gravity	EIGEN6C (120 × 120)
N-body	JPL DE405
Ocean tide	FES2004
Relativity	IERS 2003
Solid tide & pole tide	IERS 2003
Solar radiation pressure	Box-wing
Atmospheric density	DTM94 and estimating one drag parameter per 6 h
Empirical accelerations	Piecewise period at 90 min intervals
Estimated parameters	
FY-3C initial state	Position and velocity at initial epoch, X, Y, Z, V_x, V_y, V_z
Atmospheric drag	One per 360 min
Empirical accelerations	Piecewise periodical terms in the along-track, cross-track, and radial components
Receiver clock error	Each epoch as white noise
Ambiguities	Each continuous arc
Inter-system bias	Estimated as constant for dual-system POD
Estimator	
LSQ	Least squares estimation

PCO: phase correction offset; PCV: phase correction variation; ESA: European Space Agency.

4. Results

4.1. The impact of BeiDou satellite-induced code bias

Unlike the other GNSSs, BDS-2 satellites have a systematic satellite-induced code bias [22]. Using onboard BDS data, the satellite-induced code biases of GEO satellites can be modeled and corrected. Based on the multipath combination of the FY-3C onboard BDS data, the coefficients of elevation-dependent piecewise linear (PWL) models are estimated for two frequencies for every BDS satellite. Fig. 2 shows the estimated PWL model. The code bias is close to zero at low elevation and decreases gradually to the minimum value when the elevation angle is greater than 40°. Furthermore, the bias for C7I is obviously smaller than that of C2I. The maximum bias for a GEO in C2I can reach 0.5 m, and the maximum bias for C7I is relatively smaller, but still greater than 0.2 m. This result indicates that the code bias for GEO satellites should be taken into account for precise BDS applications. The bias of BDS GEO satellites for C7I is similar to that of IGSO satellites, which was also found by Zhao et al. [13]. Compared with GEO and IGSO satellites, BDS MEO satellites present the largest bias, which can exceed 1 m for C2I and reach 0.5 m for C7I.

To assess the impact of the BDS satellite-induced code bias on LEO POD, BDS and GPS dual-system onboard data from DOY

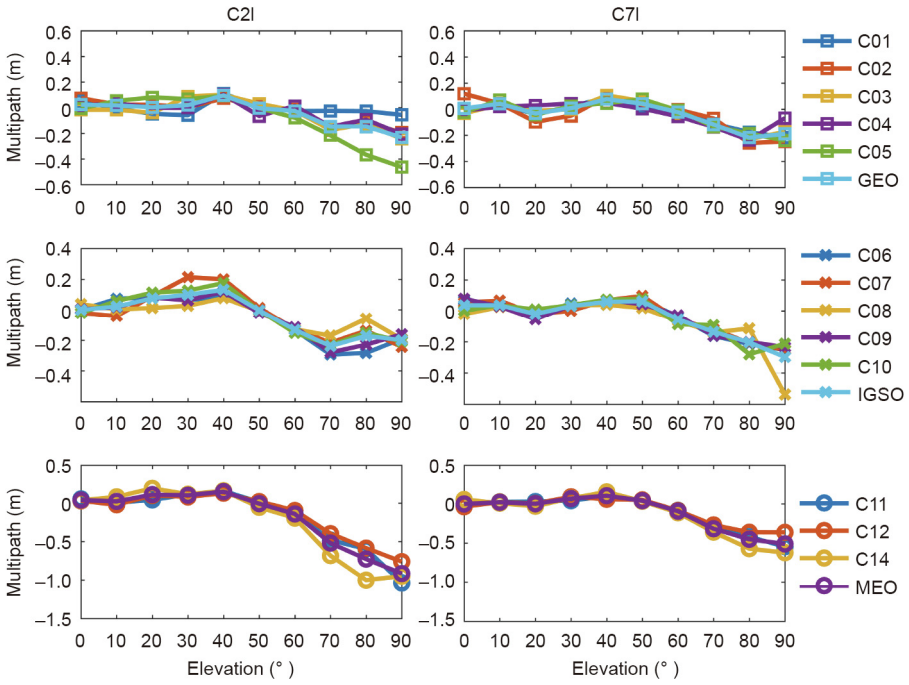

Fig. 2. Elevation-dependent PWL model values for BDS GEO, IGSO, and MEO satellites using FY-3C onboard data. Different colors represent different satellites.

080–094 in 2017 are used to perform GC (with GEO) POD for the FY-3C with and without the code bias correction. We utilize the estimated elevation-dependent PWL models based on one month of FY-3C onboard data in order to correct the code biases for BDS satellites. Fig. 3 illustrates the daily RMS of the overlapping orbit differences (OODs) for two orbit solutions. Here, the 1D RMS of the overlap differences is computed as the quadratic mean of RMS values in the along-track, cross-track, and radial components. With code bias correction, the RMS of the orbit solution can be significantly reduced. The RMS of the overlap difference is respectively reduced by 10.4%, 19.0%, and 14.9% in the along-track, cross-track, and radial components after correcting the BDS code bias. We conclude that it is important to correct the BDS code bias for LEO POD.

4.2. Orbit overlap comparison

Due to the lack of laser retroreflectors, an orbit overlap comparison is used to evaluate the accuracy of the POD. In order to avoid the impact of boundary effects on the overlap statistics,

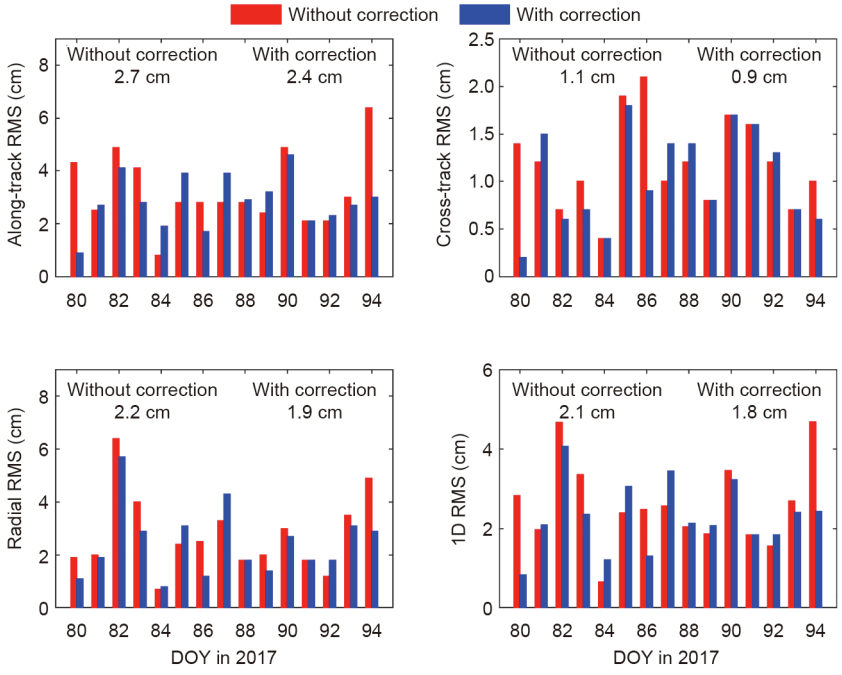

Fig. 3. Daily RMS of orbit overlapping differences for LEO POD with and without code bias correction. Red and blue bars represent the result without and with correction, respectively.

only overlap differences of 5 h (from 21:30 on the first day to 2:30 on the next day) are used in this study.

The daily RMS of the OODs of the BDS-only solution for all directions is shown in Fig. 4. The along-track component presents the largest RMS, while the cross-track component has the smallest RMS. The averaged RMS values of the OODs in the along-track, cross-track, and radial components are 204.1, 91.9, and 151.2 cm for 2013, 142.5, 65.7, and 122.6 cm for 2015, and 58.2, 34.6, and 46.5 cm for 2017, respectively. Due to the regional system of BDS and the few tracking channels for BDS, the BDS-only POD can only reach an accuracy of a few decimeters. It can also be seen that the overlapping orbit accuracy of the BDS-only solution improves gradually from 2013 to 2017. The decrease in the orbit overlap RMS can be attributed to improvements in the accuracy of BDS satellite orbit and clock products. In particular, the increased sample rate for the clock product—that is, from 5 min to 30 s—greatly reduces the accuracy degradation of the satellite clock offset caused by the mathematical interpolation, and contribute to the improvement in the accuracy of the LEO POD. Table 3 lists the corresponding statistics for the BDS-only orbit results.

Fig. 5 illustrates the daily 1D RMS of the OODs for the GC (with GEO) and GC (without GEO) POD in 2013, 2015, and 2017; the GPS-only results are also shown for comparison. Table 3 lists the corresponding statistics values. For the GPS-only solution, the averaged 1D RMS is respectively 2.0, 1.7, and 1.5 cm in 2013, 2015, and 2017, which is comparable to the accuracy of GRACE in Kang et al. [2]. The averaged 1D RMS of the dual-system solutions is relatively larger than the GPS-only result. The accuracy degradation of the dual-system schemes is mainly caused by the relatively low accuracy of BDS orbit and clock products. Compared with the GC (with GEO) POD, the orbit precision of the GC (without GEO) solution is clearly improved when BDS GEOs are excluded. The average 1D RMS of the OODs for the GC (without GEO) solution is 2.0, 1.8, and 1.3 cm in 2013, 2015, and 2017. This finding indicates that the poor quality of BDS GEO orbit and clock products can degrade the accuracy of LEO POD. It is noteworthy that in 2017, the GC (without GEO) POD achieved the smallest orbit overlap difference, which was even better than the GPS-only results. This finding demonstrates that the BDS and GPS dual-system combination can improve the accuracy of LEO POD when high-quality BDS orbit and clock products are available. Furthermore, it can be seen clearly that the orbit accuracy for both dual-system POD improves from 2013 to 2017, which is probably due to improvements in the accuracy of BDS orbit and clock products, especially the increased sampling rate for the clock product.

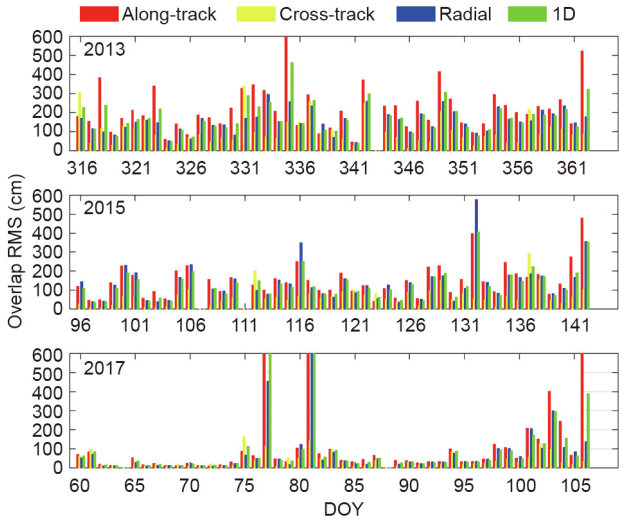

Fig. 4. Daily RMS of orbit overlap differences in all directions for the BDS-only solution.

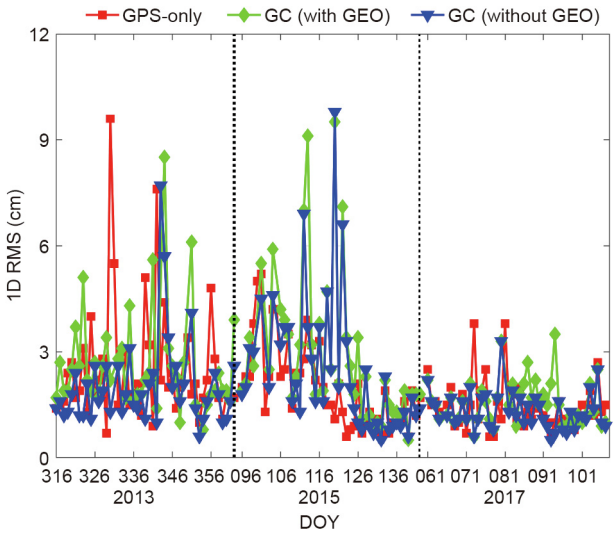

Fig. 5. Daily 1D RMS of orbit overlap differences for GPS-only, GC (with GEO), and GC (without GEO) solutions.

Fig. 6 presents the daily RMS of the orbit overlap differences for the GPS-only, GC (with GEO), and GC (without GEO) POD in 2017. It can be seen that the orbit difference in the along-track component is largest for each overlap arc, while the cross-track orbit difference is smallest. After excluding the BDS GEO, the GC combined POD for the FY-3C shows a slight improvement in the along-track and radial components compared with the GPS-only solution. Fig. 7 shows a typical time series of the number of onboard observations used for the FY-3C POD on DOY 091, 2017. It can be seen that the

Table 3
Averaged RMS of yearly orbit overlap differences in all components for BDS-only, GPS-only, GC (with GEO), and GC (without GEO) solutions.

Solution	Year	Along-track (cm)	Cross-track (cm)	Radial (cm)	1D (cm)
BDS-only	2013	204.1	91.9	151.2	150.9
	2015	142.5	65.7	122.6	115.0
	2017	58.2	34.6	46.5	47.4
GPS-only	2013	2.4	1.0	2.2	2.0
	2015	2.2	0.8	1.7	1.7
	2017	1.7	0.7	1.6	1.5
GC (with GEO)	2013	3.1	1.3	2.7	2.5
	2015	3.0	1.0	2.3	2.3
	2017	1.8	0.8	1.7	1.6
GC (without GEO)	2013	2.5	1.1	2.1	2.0
	2015	2.5	0.8	1.9	1.8
	2017	1.6	0.7	1.5	1.3

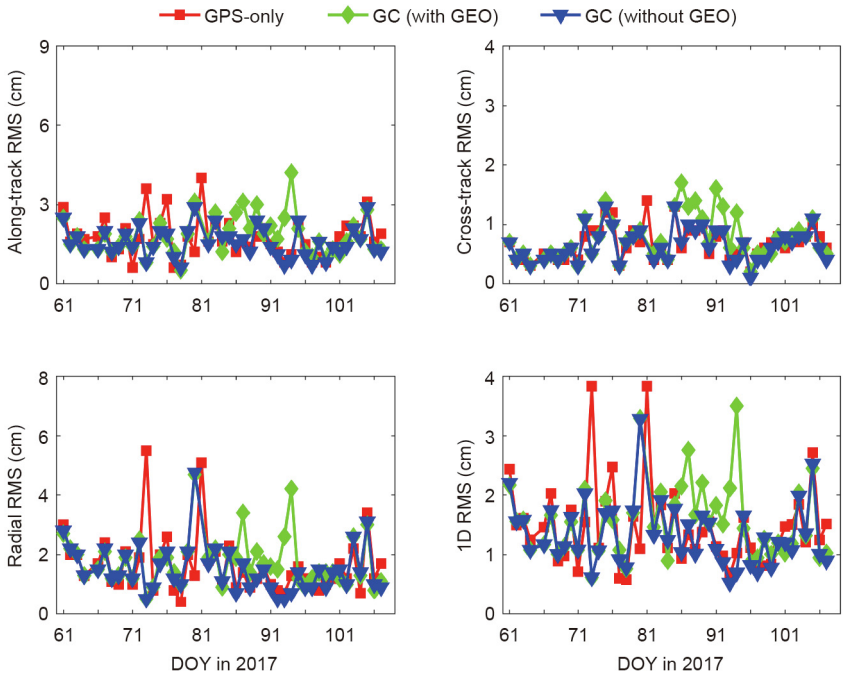

Fig. 6. Daily RMS of orbit overlap differences for GPS-only, GC (with GEO), and GC (without GEO) solutions in 2017.

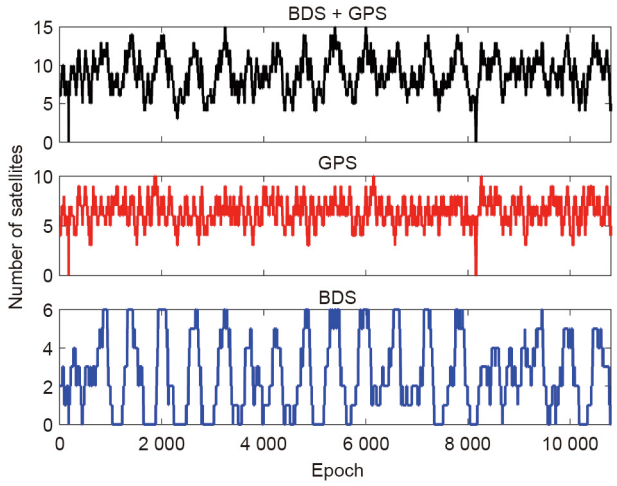

Fig. 7. Time series of number of GPS and BDS satellites used for FY-3C POD on DOY 091 in 2017.

GC combined POD can significantly increase the number of useful satellites for FY-3C POD. In some epochs, the number of satellites is as high as 15, including six BDS satellites. This result indicates that the GC combined POD can not only improve LEO POD accuracy to some extent, but also significantly improve the reliability of POD due to system redundancy.

To further assess the influence of the sample interval of the clock product on the LEO POD, BDS and GPS dual-system onboard data for DOY 080–094 in 2017 are used to perform GPS-only and GC (with GEO) POD for the FY-3C, respectively, with a clock product of 30 s and 5 min. The clock products from GFZ are used for GPS-only and GC (with GEO) solutions, respectively. Because of the lack of a MGEX clock product with a 5 min sampling interval from GFZ in 2017, we dilute the 30 s sampling interval clock product into a 5 min interval. Fig. 8 demonstrates the daily RMS of the OODs in the along-track, cross-track, radial, and 1D directions for the orbit solutions with different interval clock products; the averaged RMS values in each direction are presented at the top of each subplot. An evident improvement can be observed in the OODs for the along-track, cross-track, and radial components when a 30 s interval clock product is used. For the GPS-only solution, the RMS of the OODs with a 30 s interval clock product decreases by 50.0%, 51.6%, and 36.3% in the along-track, cross-track, and radial components, compared with the result with a 5 min clock product. For the GC (with GEO) dual-system results, the improvement is smaller than for the GPS-only solution when a high-sampling-rate clock product is used. The improvement of the GC (with GEO) solution can reach 8.8%, 9.6%, and 19.4% in the three components. This result confirms that the high-frequency clock product can reduce the accuracy degradation of the satellite clock offset due to interpolation, and improve the accuracy of LEO POD.

4.3. Residual analysis

Fig. 9 shows the RMS values of the GPS ionosphere-free carrier phase linear combination (LC) and code range linear combination (PC) residuals for GPS-only, GC (with GEO), and GC (without GEO) solutions. The average RMS values of LC residuals in 2013, 2015, and 2017 are 27.5, 19.8, and 12.6 mm for the GPS-only solution, 27.6, 20.5, and 13.1 mm for the GC (with GEO) solution and 27.3, 20.3, and 13.0 mm for the GC (without GEO) solution. The GPS LC residuals for both dual-system POD are larger than that of the GPS-only result. This finding indicates that when BDS observations are incorporated into the POD calculation, the LC residuals of GPS can be degraded due to the limited accuracy of BDS orbit and clock products. It is worth noting that the RMS of the GPS LC residuals for the GC (without GEO) and GC (with GEO) solutions shows a distinct decrease after DOY 121 in 2015. The main reason for this decrease may be that starting on DOY 123, 2015, the intervals of BDS orbit and clock products from GFZ changed from 15 min and 5 min to 5 min and 30 s. It is clear that the RMS values of the GPS LC residuals for both dual-system schemes decrease significantly from 2013 to 2017, which is due to improvement in the accuracy and sampling interval of orbit and clock products. For the

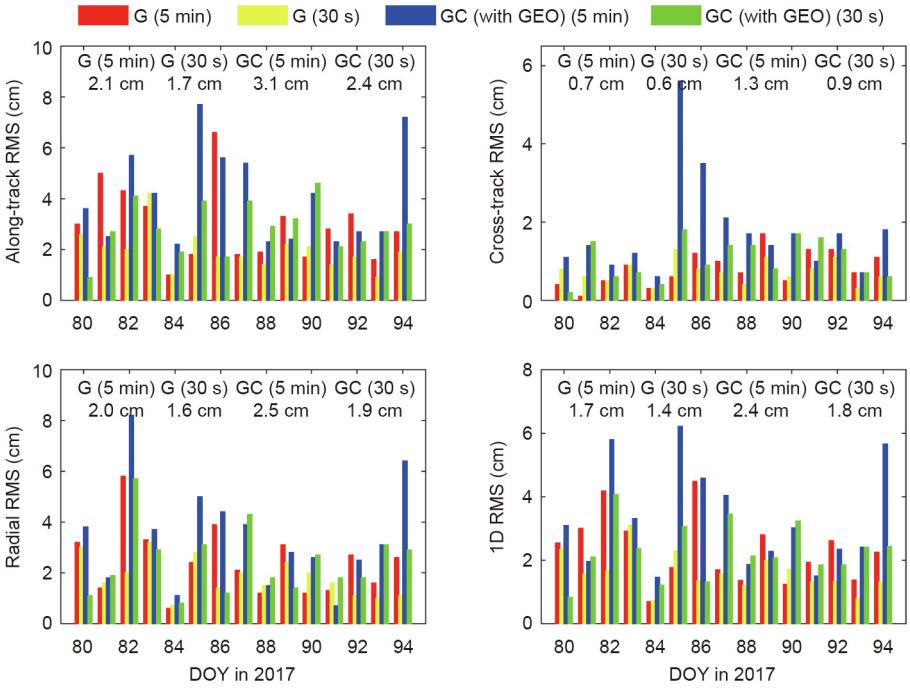

Fig. 8. Daily orbit overlap RMS for GPS-only (G) and GC (with GEO) POD with a 5 min and 30 s clock product.

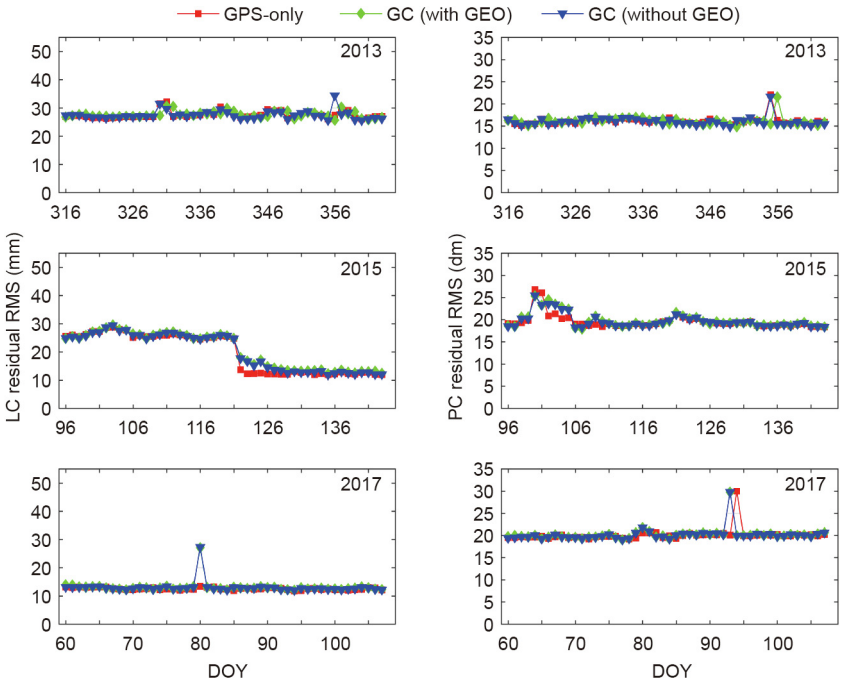

Fig. 9. RMS of GPS LC (left) and PC (right) residuals in 2013, 2015, and 2017.

PC residuals, the average RMS values in 2013, 2015 and 2017 are 16.1, 19.5, and 20.1 dm for the GPS-only solution, 16.1, 19.8, and 20.2 dm for the GC (with GEO) solution and 16.1, 19.7, and 20.3 dm for the GC (without GEO) solution. The RMS of the GPS-only POD is the smallest, while the RMS of the GC (with GEO) POD is the largest.

We calculated the RMS values of the BDS LC and PC residuals of BDS-only, GC (with GEO), and GC (without GEO) POD for individual BDS satellites from 2013 to 2017, respectively. As shown in Fig. 10, the RMS of the GEO LC residuals for the BDS-only POD is larger than that of the IGSO and MEO, which can be attributed to the low accuracy of the GEO orbit. The PC residuals RMS of the BDS satellites for BDS-only POD is around 2 m, except for the results from 2013. This may be related to the relatively low accuracy of BDS orbit and clock products in 2013. For the GC (with GEO) POD, the RMS values of the GEO LC residuals are much larger than the BDS-only results; however, the GC (with GEO) POD outperforms the BDS-only POD in orbit overlap differences, as

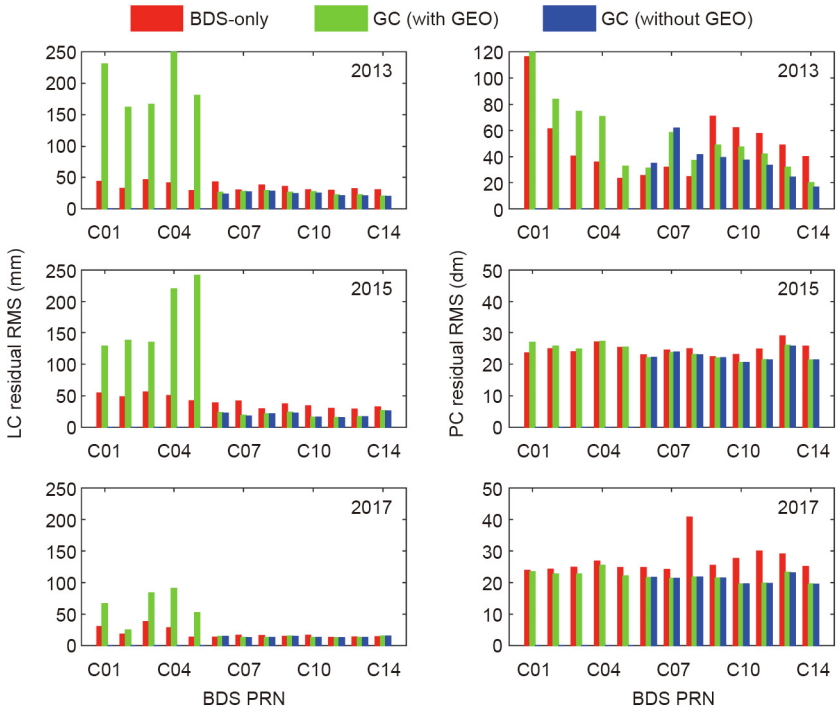

Fig. 10. RMS of BDS LC (left) and PC (right) residuals in 2013, 2015, and 2017. PRN: pseudo random noise code.

discussed in Section 4.2. This may be because the model errors of GEO satellites for the BDS-only POD are absorbed into the parameters through the estimator, which can degrade the POD precision. With BDS GEO excluded, both the PC and LC residuals for the GC (without GEO) POD decrease compared with the GC (with GEO) POD. In general, the RMS of all BDS LC and PC residuals for BDS-only and GC dual-system POD present a significant decreasing trend from 2013 to 2017 due to the accuracy improvement of BDS orbit and clock products. Taking the BDS-only solution as an example, the averaged RMS of GEO, IGSO, and MEO LC residuals for 2017 are reduced by 48.9%, 57.9%, and 55.6% in comparison with the results for 2015. This result indicates that LEO POD can greatly benefit from improvements in the accuracy and sampling interval of the BDS orbit and clock products.

5. Conclusions

This paper presented the BDS-only and GC dual-system POD for LEO in order to investigate the performance and contribution of BDS to LEO POD. Onboard BDS and GPS data collected from the FY-3C satellite during DOY 316–365 in 2013, DOY 96–145 in 2015, and DOY 61–110 in 2017 were processed.

The availability of FY-3C onboard data was analyzed first. There are many fewer BDS observations than GPS observations due to the limited channels of GNOS allocated for BDS and the regional system of BDS. Furthermore, an evident reduction can be observed in BDS data collection from 2013 to 2017. This reduction is related to an increase in data loss for BDS from 2013 to 2017, which may be due to the aging performance of the GNOS receiver.

With the code bias correction, the GC POD solution for the FY-3C showed a significant improvement in orbit overlap difference, which indicates that it is important to correct the BDS code bias for LEO POD. The GPS-only POD reaches an accuracy of a few centimeters with the OODs RMS in a 1D component of 2.0, 1.7, and 1.5 cm, respectively, in 2013, 2015, and 2017. The orbit accuracy of the BDS-only solution is much worse than the GPS-only results because BDS is still a regional navigation system at present, and the GNOS onboard the FY-3C has less than six channels allocated for the BDS signal. The GC dual-system combined POD for the FY-3C has a larger OODs RMS than that of the GPS-only solution. This indicates that the inclusion of the BDS GEOs can lead to severe accuracy degradation of LEO POD due to the poor accuracy of BDS GEO orbit and clock products. For the GC (without GEO) solution, the 1D RMS of OODs are 2.0, 1.8, and 1.3 cm in 2013, 2015, and 2017, respectively. The GC (without GEO) POD achieves a slightly better accuracy than the GPS results in all three components in 2017; the corresponding RMS of the GC (without GEO) POD in 2017 is 1.6, 0.7, and 1.5 cm in the along-track, cross-track, and radial components, respectively. These findings indicate that when high-quality BDS orbit and clock products are used, the GC combination can improve the accuracy of LEO POD in comparison with the GPS-only solution. In addition, the benefit of the BDS and GPS joint POD also lies in the reliability improvement that is simply due to system redundancy. Furthermore, an evident improvement can be found in the POD accuracy for BDS-only, GC (with GEO), and GC (without GEO) solutions from 2013 to 2017. This improvement is strongly related to the accuracy improvement of BDS orbit and clock products.

As more BDS satellites come into service and more accurate BDS orbit and clock products become available, further improvements in the accuracy of LEO POD can be expected using BDS observations and the fusion of BDS with other satellite systems.

Acknowledgements

We are very grateful to the IGS, GFZ, and WHU for providing the precise orbit and clock products of GPS and BDS. Thanks also go to the EPOS-RT/PANDA software from GFZ. This study is financially supported by the National Natural Science Foundation of China (41774030, 41974027, 41974029, and 41505030) and the Hubei Province Natural Science Foundation of China (2018CFA081). The

numerical calculations in this paper were done on the supercomputing system at the Supercomputing Center of Wuhan University.

Compliance with ethics guidelines

Xingxing Li, Keke Zhang, Xiangguang Meng, Wei Zhang, Qian Zhang, Xiaohong Zhang, and Xin Li declare that they have no conflict of interest or financial conflicts to disclose.

References

[1] Tapley BD, Ries JC, Davis GW, Eanes RJ, Schutz BE, Shum CK, et al. Precision orbit determination for TOPEX/POSEIDON. J Geophys Res Oceans 1994;99(C12):24383–404.
[2] Kang Z, Tapley B, Bettadpur S, Ries J, Nagel P, Pastor R. Precise orbit determination for the GRACE mission using only GPS data. J Geod 2006;80(6):322–31.
[3] Bock H, Jäggi A, Meyer U, Visser P, van den Ijssel J, van Helleputte T, et al. GPS-derived orbits for the GOCE satellite. J Geod 2011;85(11):807–18.
[4] van den Ijssel J, Encarnação J, Doornbos E, Visser P. Precise science orbits for the Swarm satellite constellation. Adv Space Res 2015;56(6):1042–55.
[5] Zhao Q, Guo J, Li M, Qu L, Hu Z, Shi C, et al. Initial results of precise orbit and clock determination for COMPASS navigation satellite system. J Geod 2013;87(5):475–86.
[6] Li X, Zhang X, Ren X, Fritsche M, Wickert J, Schuh H. Precise positioning with current multi-constellation Global Navigation Satellite Systems: GPS, GLONASS, Galileo and BeiDou. Sci Rep 2015;5:8328.
[7] Li P, Zhang X, Guo F. Ambiguity resolved precise point positioning with GPS and BeiDou. J Geod 2017;91(1):25–40.
[8] Xu A, Xu Z, Ge M, Xu X, Zhu H, Sui X. Estimating zenith tropospheric delays from BeiDou navigation satellite system observations. Sensors 2013;13(4):4514–26.
[9] Li M, Li W, Shi C, Zhao Q, Su X, Qu L, et al. Assessment of precipitable water vapor derived from ground-based BeiDou observations with Precise Point Positioning approach. Adv Space Res 2015;55(1):150–62.
[10] Li X, Zus F, Lu C, Dick G, Ning T, Ge M, et al. Retrieving of atmospheric parameters from multi-GNSS in real time: validation with water vapor radiometer and numerical weather model. J Geophys Res Atmos 2015;120(14):7189–204.
[11] Li M, Li W, Shi C, Jiang K, Guo X, Dai X, et al. Precise orbit determination of the Fengyun-3C satellite using onboard GPS and BDS observations. J Geod 2017;91(11):1313–27.
[12] Xiong C, Lu C, Zhu J, Ding H. Orbit determination using real tracking data from FY3C-GNOS. Adv Space Res 2017;60(3):543–56.
[13] Zhao Q, Wang C, Guo J, Yang G, Liao M, Ma H, et al. Enhanced orbit determination for BeiDou satellites with Fengyun-3C onboard GNSS data. GPS Solut 2017;21(3):1179–90.
[14] Cai Y, Bai W, Wang X, Sun Y, Du Q, Zhao D, et al. In-orbit performance of GNOS on-board FY3-C and the enhancements for FY3-D satellite. Adv Space Res 2017;60(12):2812–21.
[15] Dow JM, Neilan RE, Rizos C. The International GNSS Service in a changing landscape of Global Navigation Satellite Systems. J Geod 2009;83(3–4):191–8.
[16] Guo J, Xu X, Zhao Q, Liu J. Precise orbit determination for quad-constellation satellites at Wuhan University: strategy, result validation, and comparison. J Geod 2016;90(2):143–59.
[17] Uhlemann M, Gendt G, Ramatschi M, Deng Z. GFZ global multi-GNSS network and data processing results. In: Rizos C, Willis P, editors. IAG 150 years: Proceedings of the IAG Scientific Assembly; 2013 Sep 1–6; Postdam, Germany. Cham: Springer; 2015. p. 673–9.
[18] Schmid R, Dach R, Collilieux X, Jäggi A, Schmitz M, Dilssner F. Absolute IGS antenna phase center model igs08.atx: status and potential improvements. J Geod 2016;90(4):343–64.
[19] Rebischung P, Schmid R. IGS14/igs14.atx: a new framework for the IGS products. American Geophysical Union Fall Meeting 2016; 2016 Dec 12–16; San Francisco, CA, USA, 2016.
[20] Dilssner F, Springer T, Schönemann E, Enderle W. Estimation of satellite Antenna Phase Center corrections for BeiDou. International GNSS Service Workshop 2014; 2014 June 23–27; Pasadena, CA, USA, 2014.
[21] Berger C, Biancale R, Ill M, Barlier F. Improvement of the empirical thermospheric model DTM: DTM94—a comparative review of various temporal variations and prospects in space geodesy applications. J Geod 1998;72(3):161–78.
[22] Wanninger L, Beer S. BeiDou satellite-induced code pseudorange variations: diagnosis and therapy. GPS Solut 2015;19(4):639–48.